Proc. Natl. Acad. Sci. USA
Vol. 87, pp. 6654–6658, September 1990
Biochemistry

Antibody remodeling: A general solution to the design of a metal-coordination site in an antibody binding pocket

(antibody structure/computer modeling/metal catalysis/metalloproteins/catalytic antibodies)

VICTORIA A. ROBERTS*, BRENT L. IVERSON*, SHEILA A. IVERSON*, STEPHEN J. BENKOVIC†, RICHARD A. LERNER*, ELIZABETH D. GETZOFF*, AND JOHN A. TAINER*

*Department of Molecular Biology, Research Institute of Scripps Clinic, La Jolla, CA 92037; and †Department of Chemistry, Pennsylvania State University, University Park, PA 16802

Contributed by Stephen J. Benkovic, June 1, 1990

ABSTRACT **To develop a general approach to designing cofactor-binding sites for catalytic antibodies, we characterized structural patterns in the binding sites of antibodies and zinc enzymes. Superposition of eight sets of antibody light- and heavy-chain variable domains identified structurally conserved sites within the sequence-variable complementarity determining regions. The pattern for catalytic zinc sites included two ligands close in sequence, a sequence-distant ligand, and a main-chain hydrogen bond joining two ligands. In both the light- and heavy-chain variable domains, the stereochemistry of five structurally conserved sites general to all known antibody structures matched that of the zinc ligands of carbonic anhydrase: three residues on two hydrogen-bonded antiparallel β-strands. For one such general site, an antibody model replacing residue 34 on the first complementarity determining region of the light chain (L1) and residues 89 and 91 on the third complementarity determining region of the light chain (L3) with histidine ligands formed a zinc-binding site with an open coordination position at the bottom of the antibody binding pocket. For the anti-fluorescein antibody 4-4-20, this L1–L3 site placed the zinc ion about 4 Å from the bound fluorescein, an indicator for metal binding. This predicted zinc-binding mutant was created in the single-chain variable domain construct, expressed, and found by fluorescence quenching to bind metal ion with an affinity constant of 10^6 M^{-1}. Thus, our template-based multisite design proved successful for remodeling an antibody to contain a cofactor-binding site, without requiring further mutagenesis and screening. Combination of a specific light or heavy chain containing a catalytic metal site with a library of complementary chains raised to potential substrates or transition state analogs should greatly improve the production of catalytic antibodies with desired activities and specificities.**

Catalytic antibodies are powerful tools because the diversity of the immune response can be used to generate antibodies with specific binding properties. To date, the most common strategy for producing catalytic antibodies has involved immunization with carefully designed synthetic antigens such as transition state analogs to elicit antibodies that catalyze bond cleavage (see ref. 1 and references therein), electrostatically or sterically complementary antigens to induce specific catalytic residues in the binding pocket (2, 3), and peptide-linked metal cofactors to generate cofactor-assisted catalytic antibodies (4). Alternatively, catalytic antibodies can be produced from existing noncatalytic antibodies by the covalent attachment of cofactors (5) and by single-site mutagenesis (6).

To reduce the currently required extensive screening and to increase the success rate for obtaining catalytic antibodies, we have chosen to develop a general approach for remodeling antibody complementarity determining regions (CDRs) to create predetermined cofactor-binding sites. Since the cloning and expression of the antibody repertoire in microorganisms allows separate light- and heavy-chain libraries to be combined in random pairs (7, 8), we can combine one chain designed to have a cofactor-binding site with a library of complementary chains raised against an appropriate substrate analog. These chimeric antibodies would mimic enzymes in having both a catalytic site, designed by site-directed mutagenesis, and a binding site, created by the immune system. Here, we report the initial step towards this goal, the development and implementation of a general strategy for designing potentially catalytic metal cofactor sites in antibody light or heavy chains. By using our knowledge of the consensus three-dimensional structure of antibodies, multisite mutants can be modeled and then constructed by antibody engineering experiments (9, 10).

We chose to design and create a zinc-binding antibody because many useful reactions, including hydrolysis, are catalyzed by zinc-containing enzymes (11) and because requirements for a catalytic zinc-binding site can be analyzed from the solved three-dimensional structures of zinc enzymes. Since hydrolysis in zinc enzymes requires a vacant metal coordination site for an activated water molecule, our remodeled antibody was designed to have three ligands that would position the zinc and its solvent-exposed site to interact with bound antigen.

MATERIALS AND METHODS

The structures of antibody variable domains of HyHEL5, HyHEL10, Newm, J539, HEd10, and Kol, available from the Brookhaven National Laboratory Protein Data Bank (12), and D1.3 (13) were compared by superimposing individual light-chain variable domains (V_L) and heavy-chain variable domains (V_H) onto the corresponding domains of McPC603 (12). A slightly modified set of the common β-sheet framework residues of Chothia and Lesk (14) was used to define the one-to-one correspondence of the superposition. In the numbering scheme of Kabat *et al.* (15), these were V_L residues 4–6, 9, 11–13, 19–25, 33–49, 53–55, 61–76, 84–90, and 97–107 and V_H residues 3–12, 17–25, 33–52, 56–60, 68–82, 88–95, and 102–112. We excluded V_L residues 10 and 106A, because these residues are deleted in some sequences. The crystallographic structure (16) of the anti-fluorescein antibody 4-4-20 was not included in our data base but used to test it. A search of the Brookhaven National Laboratory Protein Data Bank provided crystallographic structures of five catalytic

The publication costs of this article were defrayed in part by page charge payment. This article must therefore be hereby marked "*advertisement*" in accordance with 18 U.S.C. §1734 solely to indicate this fact.

Abbreviations: V_L and V_H, variable domains of light and heavy chains; Fv, variable domain consisting of V_L and V_H; CDR, complementarity determining region; L*n* and H*n*, *n*th CDR of V_L and V_H; CAB, carbonic anhydrase.

zinc-containing proteins: carbonic anhydrase (CAB) (17), carboxypeptidase A (18), superoxide dismutase (19), alcohol dehydrogenase (20), and thermolysin (21).

The CDRs of the antibodies were examined for all main-chain hydrogen bonds, defined by a maximum distance of 3.5 Å between nitrogen and oxygen atoms. The program INSIGHT (Biosym Technologies, Inc., San Diego, CA) was used to superimpose the C^{α} and C^{β} atoms of zinc ligands onto the antibody CDRs, to examine and analyze the resulting models, and to create Figs. 1*B* and 2.

A four-site mutant (QM212) of the single-chain variable region domain (Fv) construct (4-4-20/202'; Genex) was made by cloning and expression in *Escherichia coli* according to previously described protocols (9). Metal binding was probed by fluorescence quenching of tryptophan residues, which occur in or near the CDRs, and by examination of the fluorescence spectrum of fluorescein as detailed elsewhere (31).

RESULTS AND DISCUSSION

Motifs in Antibody CDRs and Metalloenzyme Catalytic Zinc-Binding Sites. The design of a functional site that can be incorporated into any member of a family of proteins requires the characterization of common structural features shared by all members of the family. Superposition of the V_L and V_H framework of seven antibodies onto the McPC603 antibody revealed that the conserved β-sheet structure of the framework region was continued into the CDRs in all structures (Fig. 1*A*). These CDR regions had the characteristics required for a general potential cofactor site—conserved predictable structure with allowed sequence variability, so that mutations are unlikely to perturb the overall structure. The first CDR of V_L (L1) is a Greek key loop joining nonadjacent β-strands across the end of the β-barrel, L2 is an extended strand and β-turn (except in Newm), and L3 is a continuation of two adjacent framework β-strands with a variable connecting loop. The first CDR of V_H (H1) is an extended β-strand, H2 is two adjacent β-strands connected by a variable loop, and H3 is a continuation of two β-strands with a highly variable connecting loop. Overall, portions of L1, L3, H2, and H3 showed the most conformational variability and were the most likely candidates for inducible complementarity and antigen binding.

A search of crystallographic structures in the Brookhaven National Laboratory Protein Data Bank (12) revealed several catalytic zinc-binding motifs. Three residues, predominantly histidine, but also glutamate, aspartate, and cysteine, coordinated the metal ion in a roughly tetrahedral geometry. Generally at least two of the ligands in zinc-binding proteins were close together in the protein sequence, as also found by a recent independent study based on sequence analysis (11). We have found an additional important shared structural characteristic of the zinc-binding sites not shown by sequence analysis. In most catalytic sites, main-chain hydrogen bonds connected two of the zinc-ligating residues.

The metal ligand stereochemistry of these zinc-containing enzymes provided templates representing the three common secondary structure motifs with hydrogen-bonded main chains—adjacent β-strands, β-turns, and α-helices (Fig. 1*B*). The zinc ligands of CAB (17), representing the β-strand motif, were three of four residues in two adjacent hydrogen-bonded pairs joining two antiparallel β-strands. The two ligands on one β-strand were separated by one intervening residue. All four of the residues in the two adjacent hydrogen-bonded pairs had their C^{α}—C^{β} bonds pointing towards the zinc ion and the open coordination position, so appropriate substitution of any three of the four side chains could create a potential zinc-binding site. In carboxypeptidase A (18) and superoxide dismutase (19), two of the zinc ligands, separated by two intervening residues, were in the 1 and 4 positions of a type I β-turn. In the α-helical motif seen in thermolysin (21), elastase (23), and neutral protease (24), two histidine ligands, separated by three intervening residues, were linked by an α-helical, main-chain hydrogen bond. The third ligand was on an adjacent antiparallel helix.

The main-chain hydrogen-bonding constraint in all of these structures caused two of the ligating side chains to extend away from the backbone in approximately the same direction, positioning the zinc-ligating atoms near to each other. Only alcohol dehydrogenase (20), which differs from the other catalytic sites in both ligand type and sequential spacing (11), contained a catalytic zinc site lacking two hydrogen-bonded ligands. Thus, the available protein structures with catalytic zinc sites showed that a main-chain hydrogen bond

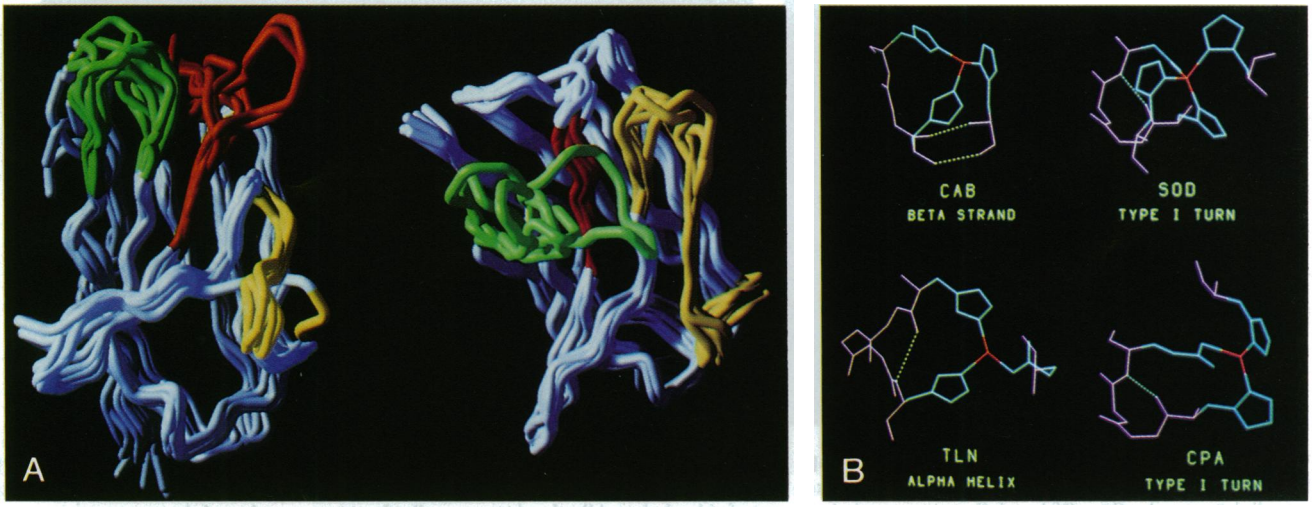

FIG. 1. Motifs in antibody CDRs and enzyme zinc-binding sites. (*A*) Superposition of the framework Fv regions (silver) for the antibodies McPC603, D1.3, HyHEL5, HEd10, Newm, Kol, and J539, showing the C^{α} backbones of V_L (*Left*) and V_H (*Right*) with CDRs L1 and H1 (red), L2 and H2 (yellow), and L3 and H3 (green). In this view the two halves of the binding site (top) face forward. Although the CDRs show much more structural variation than the framework regions, all the antibodies shared the β-strand structure that extends from the framework into the CDRs. The figure was rendered using the programs AMS and MCS (22) and displayed on a Sun TAAC-1. (*B*) Zinc-binding sites in CAB (17), superoxide dismutase (SOD) (19), carboxypeptidase A (CPA) (18), and thermolysin (TLN) (21) showing the main-chain hydrogen-bond patterns of the ligating residues and the intervening structure (β-strand, β-turn, and α-helix) between the sequentially close ligands.

was important for proper ligand arrangement, whereas the major backbone conformation, β-sheet, β-turn, or α-helix, was variable. Therefore, we examined the CDRs of the available antibody structures for main-chain hydrogen-bonded residues that would make up two of the three zinc ligands. The metalloenzyme zinc-binding sites were then superimposed onto these antibody sites to provide three-dimensional templates for zinc sites in antibodies.

Design of General Zinc-Binding Sites in Antibodies. Within the V_L and V_H CDRs, 11 sites for metal coordination were identified (Table 1), which together involve all six CDRs. Only one example each of hydrogen-bonded ligands with turn or α-helical secondary structures was found. A general β-turn site on L2 placed the zinc ion between L2 and H3. A short helix in L1 (λ light chain) should accommodate the zinc-binding site, placing an open coordination site for a water molecule between L1 and L3. However, the β-strand motif in CAB provided the best template for building general metalloantibody sites because it mimicked conserved structural features of the CDRs deep in the antibody binding pocket. For the eight antibodies examined, the CDRs, which consist of 50–60 residues per antibody, contained nine general sites with stereochemistry similar to CAB (Table 1). Five of these sites included the important hydrogen-bonding feature: two placed the zinc in the center of the binding pocket (the L1–L3 site and the H1–H3 site), one placed the zinc between L1 and L3 (an L3 site), and two placed the zinc between H2 and L3 (the two H2 sites).

We chose to test our design approach using the L1–L3 site, which consisted of residues 34, 89, and 91 [Kabat numbering (15)]. This site satisfied all of our design requirements: (*i*) a structurally conserved, sequence-variable region common to all antibodies, (*ii*) a pair of hydrogen-bonded residues, and (*iii*) three ligands that would position the zinc and its solvent-exposed site to interact with bound antigen. The main-chain hydrogen bond between residue 34, the last residue of L1, and residue 89, the first residue of L3, continued the framework antiparallel β-sheet structure into the CDRs. The main-chain and side-chain positions in the L1–L3 site strongly resembled the zinc-binding site of CAB (Fig. 2*A*). In all antibodies, the C^α and C^β atoms of residues 89, 91, and 34 extended out from one side of the β-sheet with stereochemistry similar to residues 94, 96, and 119 of the enzyme. In the antibodies D1.3, HyHEL10, J539, and McPC603, the β-

Table 1. Template-derived zinc-binding sites in antibody CDRs

Antibody ligand positions	Zinc site location*	H bond†	Other ligands‡
β-Strand			
L1 (34), L3 (89, 91)	Center	34–89	L1 (32)
L3 (90, 92, 97)	L1 and L3	90–97	L3 (95)
L3 (89, 91, 96)	Center	91:96	
H1 (33, 35), H3 (95)	Center	33–95	
H1 (33, 35), H2 (50)	Center	35:50	H2 (52)
H1 (31, 33), H2 (52)	Center	33:52	
H2 (50, 52, 58)	H2 and L3	50–58	H2 (56)
H2 (50, 58, 60)	H2 and L3	50–58	
H3 (95, 101§)	Center	95:101§	H3 (100I)¶
β-Turn			
L2 (50, 53, 55)	L2 and H3	50 · · · 53	
α-Helix			
L1 (27D, 29)‖	Above site	27D · · · 29	L3 (93)

Numbering for residues is according to Kabat (15).
*The zinc ion was either positioned in the center of the binding pocket between L3 and H3 (center) or between the two CDRs indicated.
†Residues with strongly conserved hydrogen bonds are indicated by "–", and those with N—O distances greater than 3.5 Å in some antibodies are indicated by "· · ·". Non-hydrogen-bonded pairs of residues that occur in β-strands are indicated by ":".
‡Either a potential replacement for any of the three ligands or a possible third ligand if only two are listed.
§Residue 101 or the preceding residue of H3 (i.e., residue 100K of McPC603).
¶Numbered according to McPC603.
‖The site applies only to the variable domain of the λ light chain.

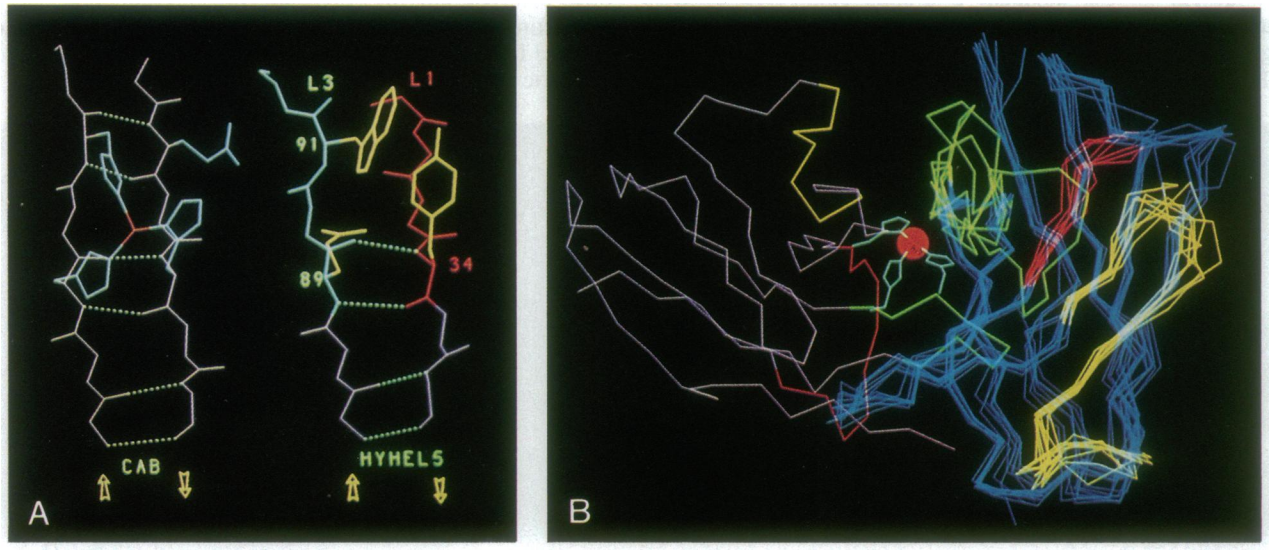

FIG. 2. Building the zinc site of CAB onto the L1–L3 site of HyHEL5. (*A*) Comparison of the zinc ligands (light blue) of CAB (17) (*Left*) with the residues (yellow) of the L1 (red)–L3 (green) site in the HyHEL5 structure (25) (*Right*), showing the similarity of hydrogen-bonding antiparallel β-strands, C^α—C^β bond directions, and placement of side chains. All other known antibody structures shared the arrangement seen in HyHEL5 in this region. Arrows indicate the direction of the polypeptide chain. (*B*) The general L1–L3 zinc site allows combination with a library of heavy chains to form a zinc-cofactor site in the antibody Fv. The model of the HyHEL5 Fv C^α backbone with the CAB zinc-binding site built into V_L (magenta) is combined with superimposed C^α backbones of V_H (blue) of antibodies HyHEL5, HyHEL10, Newm, J539, HEd10, Kol, D1.3, and McPC603. CDRs L1 and H1 are red, L2 and H2 are yellow, and L3 and H3 are green. The C^α and C^β atoms of CAB zinc-ligating residues 94, 96, and 119 were superimposed onto the corresponding atoms of HyHEL5 V_L residues 89, 91, and 34, respectively (root-mean-square deviation between the two structures of 0.57 Å for the six atoms). The three histidine ligands (light blue side chains) placed the zinc ion (red sphere) at the bottom of the binding pocket between L3 and H3.

structure extended further up L1 and L3, providing a second hydrogen-bonded pair between residues 32 and 91, further mimicking CAB. Although the side chain of L1 residue 32 pointed up out of the antibody binding site rather than into it, the energy gained by zinc binding should be sufficient to position residue 32 as a zinc ligand. Thus, the conserved structural pattern of the L1–L3 site seen in all antibody structures suggested that replacement of any three of residues 32, 34, 89, and 91 by histidines should create a zinc-binding site in the antibody binding pocket. Superposition of zinc-ligating residues His-94, -96, and -119 of CAB (17) onto residues Gln-89, Trp-91, and Tyr-34 of the antibody HyHEL5 (25) revealed that the zinc ion would be positioned near the center of the bottom of the binding pocket in an apparently ideal orientation to act as a catalytic cofactor (Fig. 2*B*). Residue replacement and metal binding should not have a significant effect on the folding of the CDRs, because amino acid substitutions are not uncommon for these four antibody residue positions. For example, Tyr-34 is replaced by a histidine in both antibodies J539 and HyHEL10. However, even apparently conservative mutations could result in significant conformational changes if CDR residues have unidentified structural functions (26).

A V_L metal site positioned deep in the pocket, such as the L1–L3 site, would interact with a substrate whose binding site would be formed by other antibody residues, especially those from the highly variable H3 (Fig. 2*B*). Because of H3 variability (Fig. 1*A*) and its involvement in many antigen–antibody interactions (13, 16), chimeric antibodies composed of substrate-specific heavy chains and our metal-binding light chain should bind substrate adjacent to the metal ion, thereby allowing catalysis.

Design of a Specific Zinc-Binding Site in an Anti-Fluorescein Antibody. To investigate L1–L3 metal site, we built a model based upon the crystal structure of the complex of fluorescein bound to the anti-fluorescein antibody 4-4-20 (16). Since changes in the fluorescence spectrum of fluorescein should occur if both metal ion and antigen bind simultaneously, remodeling the anti-fluorescein Fv should be an excellent test for our template-based design. The 4-4-20 antibody structure, not used in our analysis of potential zinc-binding sites, had the predicted common structural elements seen in our antibody data base. As in McPC603, the L1–L3 site of 4-4-20 had two pairs of hydrogen-bonded residues, residues 34 and 89 and residues 32 and 91. Replacement of Arg-34 and Ser-91 by histidine residues was expected to decrease the fluorescein binding constant of the mutant relative to the wild-type antibody, because these two residues are hydrogen bonded to the hydroxyl of fluorescein in the crystal structure. Superposition of the C^α and C^β atoms of CAB His-119, -94, and -96 onto the corresponding atoms of V_L Arg-34, Ser-89, and Ser-91 placed the zinc ion at the bottom of the antibody binding pocket with its solvent-exposed surface close to the hydroxyl of fluorescein, such that the van der Waals surfaces of these two atoms almost touched (Fig. 3). Potentially unfavorable steric interactions found in the model between His-89 in the introduced zinc site and the hydroxyl of framework residue Tyr-36 were eliminated by conservative replacement of Tyr-36 with leucine, which occurs here in other antibodies.

To test the template-based, multisite design strategy, a mutant of the Fv single-chain variant (Genex) of the antibody 4-4-20 was made and characterized as described in a separate report (31). Briefly, this four-site (His-34, His-89, His-91, and Leu-36) mutant, called QM212, was expressed, cloned in *E. coli*, purified, and examined for metal binding by fluorescence quenching (copper, but not zinc, quenches fluorescence). The fluorescence spectrum of fluorescein was not perturbed by the addition of copper in the wild-type antibody but was perturbed in the mutant, indicating that the metal ion

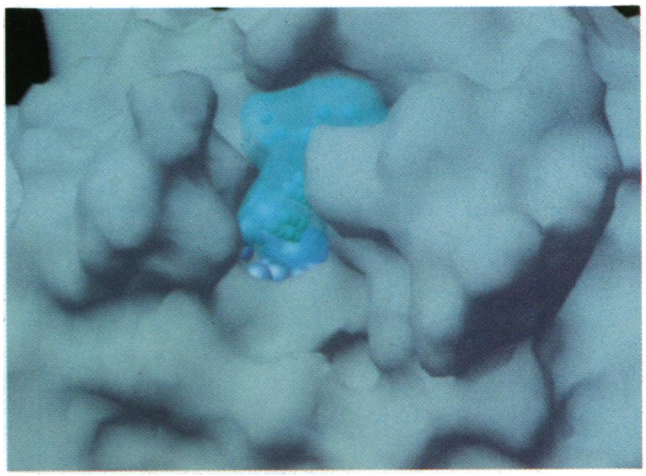

FIG. 3. Model of the antibody 4-4-20 Fv, complexed with fluorescein, with the CAB zinc site built in. The solvent-accessible surfaces of fluorescein (center, light blue and transparent) and the antibody Fv (gray) excluding the side chains of mutated V_L residues 34, 89, and 91 were made with the program AMS (22) and displayed with AVS on a Stardent mini supercomputer. Superposition of the C^α and C^β atoms of CAB (17) His-119, -94, and -96 onto the corresponding atoms of Arg-34, Ser-89, and Ser-91 of the 4-4-20 (16) Fv gave a root-mean-square deviation between the two structures of 0.37 Å for the six atoms. The superposition placed the zinc atom (blue sphere) and its ligands (silver spheres) at the bottom of a cleft in the antibody binding site. The zinc ion is about 4 Å from the hydroxyl of fluorescein and from the carboxylate oxygen atoms of V_H Asp-101.

was bound close to the fluorescein. The six tryptophan residues in the Fv of 4-4-20 all clustered about the binding site, providing an internal indicator for metal binding. For the wild-type antibody, the addition of copper caused only slight tryptophan fluorescence quenching, as would be expected for copper in solution, but, for the mutant, copper caused >80% quenching, indicating that the copper ion binds near the tryptophan residues. Competitive binding studies show that QM212, like CAB, has a preference for copper over zinc over cadmium binding (31). By Scatchard analysis (Fig. 4), we have determined the binding constant for copper to QM212 to be about 10^6 M^{-1}.

Implications for Catalytic Antibody Design. The catalytic and binding sites of enzymes are usually well-conserved, whereas the binding sites of antibodies, made up of the CDRs, are inherently variable. Examination of the structures of catalytic zinc ion sites in proteins indicated a highly conserved stereochemistry, including a specific main-chain hydrogen bond between two of the three ligands. Examination of antibody structures showed that regions of the CDRs have highly variable conformations determined by sequence and environment. Both metal and antigen binding may induce conformational rearrangements (27, 28) of these regions. However, the structurally conserved, but sequence variable, regions of the CDRs that we have identified here should tolerate mutation without significant conformational perturbation. These regions were compared with the structural patterns of zinc-binding sites in enzymes using a "template-based" approach to create metal-binding sites that are generally applicable to all antibodies.

To demonstrate that knowledge of the structural chemistry of protein metal sites and antibody CDRs is sufficient to construct metal-binding antibodies in a single design step, we selected and tested one general V_L site (Table 1, first entry). The resulting metalloantibody mutant demonstrated that structural patterns can provide a template for a successful design of a multisite mutant, without extensive screening or rescue of the site by either random mutagenesis or antibody

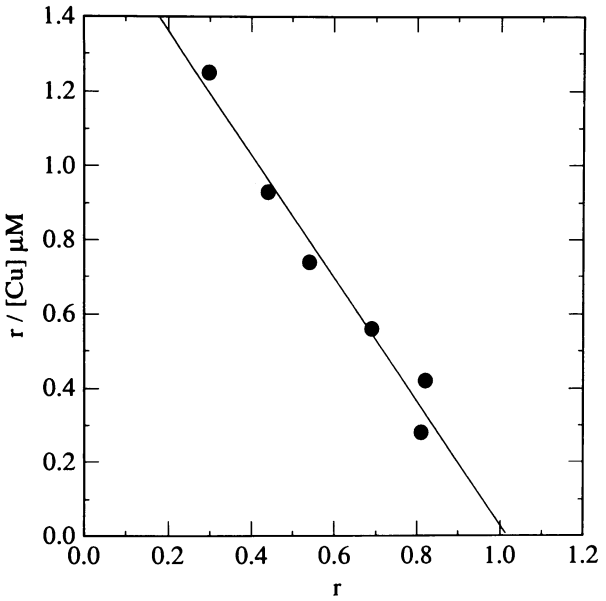

FIG. 4. Scatchard plot of copper binding to the four-site mutant QM212, where r is the ratio of protein with bound copper to total protein and [Cu] is the concentration of free copper. To 150 nM protein (Lowry determination) in 1.0 ml of 2.0 mM Mes (pH 6.2) at 20°C was added 2- to 8-μl samples of 125 μM $CuCl_2$. After gentle mixing with a suspended teflon stirring bar and a 5-min equilibration, the tryptophan fluorescence at 345 nm was monitored by using excitation at 292 nm in a Shimadzu RF5000U spectrofluorophotometer. A quenching maximum of 0.5 (determined separately) was used. Data were corrected for mixing effects and background copper quenching by comparison with identical experiments conducted on the wild-type 4-4-20/212 protein (9). Linear regression gave a binding constant of copper to QM212 of 1.7×10^6 M^{-1} under these conditions.

combinatorics. Given that the introduction of three histidine residues into an antibody created a metal-binding site without disrupting protein folding, the site could be further optimized by considering secondary environmental effects (29) in our model, such as precise ring alignment requirements or the satisfaction of additional side-chain hydrogen bonds. This process of characterizing and testing should increase fundamental knowledge of enzyme catalysis by defining the requirements for cofactor binding and environment.

The ability to design metal-binding sites in structurally conserved areas of the CDRs should have broad implications for catalytic antibody design. For example, humanized monoclonal antibodies (10) directed against medically important targets may be modified, while retaining binding, to achieve peptide bond cleavage or other chemical reactions. The ability to construct zinc coordination sites in antibodies as shown here and to raise anti-peptide antibodies that cross-react with flexible, exposed regions of proteins as shown previously (30) suggests that sequence-specific, site-directed proteases may be obtained by adding a zinc-binding site to the appropriate antibody. Also, combining metal-binding light chains with various heavy-chain libraries raised to different substrates will extend this method to a wide variety of important reactions that use a metal cofactor. Finally, although we have focused on zinc metalloenzymes, antibodies could be remodeled to bind other cofactors after determining the stereochemical preferences for the cofactor sites. Thus, to design superior catalytic antibodies, immune selection to optimize binding can be combined with template-based design to optimize catalysis.

We thank Michael Pique for contributions to the computer graphics, Genex for the 4-4-20/202' single-chain antibody Fv plasmid, Drs. R. Poljak and A. Edmundson for their Fab coordinates, and Drs. A. Feinstein and D. Stout for helpful discussions. This work was funded in part by National Institutes of Health Grants RO1 GM37684 (E.D.G.) and RO1 GM 39345 (J.A.T.) and Fellowship F32GM-1204702 (S.A.I.).

1. Lerner, R. A. & Benkovic, S. J. (1990) *Chemtracts-Org. Chem.* **3**, 1–36.
2. Skokat, K. M., Leumann, C. J., Sugasawara, R. & Schultz, P. G. (1989) *Nature (London)* **338**, 269–271.
3. Janda, K. D., Weinhouse, M. I., Schloeder, D. M., Lerner, R. A. & Benkovic, S. J. (1990) *J. Am. Chem. Soc.* **112**, 1274–1275.
4. Iverson, B. L. & Lerner, R. A. (1989) *Science* **243**, 1184–1188.
5. Pollack, S. J. & Schultz, P. G. (1989) *J. Am. Chem. Soc.* **111**, 1929–1931.
6. Baldwin, E. & Schultz, P. G. (1989) *Science* **245**, 1104–1107.
7. Huse, W. D., Sastry, L., Iverson, S. A., Kang, A. S., Alting-Mees, M., Burton, D. R., Benkovic, S. J. & Lerner, R. A. (1989) *Science* **246**, 1275–1281.
8. Ward, E. S., Güssow, D., Griffiths, A. D., Jones, P. T. & Winter, G. (1989) *Nature (London)* **341**, 544–546.
9. Bird, R. E., Hardman, K. D., Jacobson, J. W., Johnson, S., Kaufman, B. M., Lee, S.-M., Lee, T., Pope, S. H., Riordan, G. S. & Whitlow, M. (1988) *Science* **242**, 423–426.
10. Riechmann, L., Clark, M., Waldmann, H. & Winter, G. (1988) *Nature (London)* **332**, 323–327.
11. Vallee, B. L. & Auld, D. S. (1990) *Proc. Natl. Acad. Sci. USA* **87**, 220–224.
12. Bernstein, F. C., Koetzle, T. F., Williams, G. J. B., Meyer, E. F., Jr., Brice, M. D., Rodgers, J. R., Kennard, O., Shimanouchi, T. & Tasumi, M. (1977) *J. Mol. Biol.* **112**, 535–542.
13. Amit, A. G., Mariuzza, R. A., Phillips, S. E. V. & Poljak, R. J. (1986) *Science* **233**, 747–753.
14. Chothia, C. & Lesk, A. M. (1987) *J. Mol. Biol.* **196**, 901–917.
15. Kabat, E. A., Wu, T. T., Reid-Miller, M., Perry, H. M. & Gottesman, K. S. (1987) *Sequences of Proteins of Immunological Interest* (U.S. Dept. HHS, Washington).
16. Herron, J. N., He, X., Mason, M. L., Voss, E. W., Jr., & Edmundson, A. B. (1989) *Proteins* **5**, 271–280.
17. Kannan, K. K., Notstrand, B., Fridborg, K., Lövgren, S., Ohlsson, A. & Petef, M. (1975) *Proc. Natl. Acad. Sci. USA* **72**, 51–55.
18. Rees, D. C., Lewis, M. & Lipscomb, W. N. (1983) *J. Mol. Biol.* **168**, 367–387.
19. Tainer, J. A., Getzoff, E. D., Richardson, J. S. & Richardson, D. C. (1983) *Nature (London)* **306**, 284–287.
20. Brandén, C. I., Jörnvall, H., Eklund, H. & Furugren, B. (1975) in *Enzymes*, ed. Boyer, P. D. (Academic, New York), 3rd Ed., Vol. II, p. 103.
21. Holmes, M. A. & Matthews, B. W. (1982) *J. Mol. Biol.* **160**, 623–639.
22. Connolly, M. L. (1985) *J. Mol. Graph.* **3**, 19–24.
23. Thayer, M. M. (1989) Ph.D. thesis (University of Colorado, Boulder, CO).
24. Pauptit, R. A., Karlsson, R., Picot, D., Jenkins, J. A., Niklaus-Reimer, A.-S. & Jansonius, J. N. (1988) *J. Mol. Biol.* **199**, 525–537.
25. Sheriff, S., Silverton, E. W., Padlan, E. A., Cohen, G. H., Smith-Gill, S. J., Finzel, B. C. & Davies, D. R. (1987) *Proc. Natl. Acad. Sci. USA* **84**, 8075–8079.
26. Chien, N. C., Roberts, V. A., Giusti, A. M., Scharff, M. D. & Getzoff, E. D. (1989) *Proc. Natl. Acad. Sci. USA* **86**, 5532–5536.
27. Getzoff, E. D., Geysen, H. M., Rodda, S. J., Alexander, H., Tainer, J. A. & Lerner, R. A. (1987) *Science* **235**, 1191–1196.
28. Getzoff, E. D., Tainer, J. A., Lerner, R. A. & Geysen, H. M. (1988) *Adv. Immunol.* **43**, 1–98.
29. Argos, P., Garavito, R. M., Eventoff, W. & Rossman, M. G. (1978) *J. Mol. Biol.* **126**, 141–158.
30. Tainer, J. A., Getzoff, E. D., Alexander, H., Houghten, R. A., Olson, A. J., Lerner, R. A. & Hendrickson, W. A. (1984) *Nature (London)* **312**, 127–133.
31. Iverson, B. L., Iverson, S. L., Roberts, V. A., Getzoff, E. D., Tainer, J. A., Benkovic, S. J. & Lerner, R. A. (1990) *Science*, in press.